An In-depth Study of Offset Quadrature Phase-shift Keying

An In-depth Study of Offset Quadrature Phase-shift Keying

By

Michael Rice

Cambridge
Scholars
Publishing

An In-depth Study of Offset Quadrature Phase-shift Keying

By Michael Rice

This book first published 2025

Cambridge Scholars Publishing

Lady Stephenson Library, Newcastle upon Tyne, NE6 2PA, UK

British Library Cataloguing in Publication Data
A catalogue record for this book is available from the British Library

ISBN: 978-1-0364-5864-5
ISBN (Ebook): 978-1-0364-5865-2

Table of Contents

1 A Short History of Offset QPSK 1

2 Description and Properties 21
Preliminaries 21
Time-Domain Description 29
Pulse Shapes 30
Symbols 32
Benefits of the Timing Offset 33
Frequency-Domain Description 41
Detection in the AWGN Environment 47
Filtered OQPSK With Nonlinear Amplifiers. 58
Summary and Conclusions 71

3 Carrier Phase Synchronization 73
Problem Formulation 74
Data-Aided Phase Estimator 75
The Feedforward Carrier Phase Estimator 77
Feedforward Performance Analysis 78
The Feedback Carrier Phase Estimator. 82
The Data-Aided Carrier Phase PLL 84
PLL Performance Analysis 88
Non-Data-Aided Phase Estimator 99
Problem Formulation 99
The Non-Data-Aided Carrier Phase PLL 101
PLL Performance Analysis 104
Practical Realizations of the Carrier Phase PLL 109
Summary and Conclusions 111

4 Symbol Timing Synchronization 115
Problem Formulation 117
Data-Aided Timing Estimator. 117
Search 1: Finding the Maximizer of $\Lambda_{\mathrm{DA}}(\tau)$ Using The Dichotomous Search 121
Search 2: Finding the Maximizer of $\Lambda_{\mathrm{DA}}(\tau)$ Using Interpolation 129
Search 3: Finding the Zero of $\dot{\Lambda}_{\mathrm{DA}}(\tau)$ Using the Bisection Search 134
Search 4: Finding the Zero of $\dot{\Lambda}_{\mathrm{DA}}(\tau)$ Using A Sequential Search 139
The Data-Aided Symbol Timing PLL: Description . . 143
The Data-Aided Symbol Timing PLL: Performance . . 145
Non-Data-Aided Timing Estimator 159
The Non-Data-Aided Symbol Timing PLL 162
Practical Realizations of Symbol Timing Synchronizers. . 168
Timing Adjustments 1: The Polyphase Filterbank . . 169
Timing Adjustments 2: Interpolation Filters. 178
Interpolation Control in the Symbol Timing PLL . . . 192
Timing Error Detectors 217
Summary and Conclusions 237

5 Joint Carrier Phase and Symbol Timing Synchronization 241
Problem Formulation 241
Data-Aided Estimator 242
Joint Feedforward Estimator 245
Joint Feedback Estimator: Joint Carrier Phase and Symbol Timing PLLs. 250
Non-Data-Aided Estimator 268
Derivation 268
The Non-Data-Aided Joint PLL 269
Ambiguity Resolution 279
Summary and Conclusions 281

6 Differential Detection 283
Preliminaries 285
Differential Encoder 1 287

Differential Encoder 2 290
Problem Formulation 291
A Survey of Approaches 292
Defly, Lecours, Boutin (1989) 292
Matched Filtering 297
Kaleh (1989) 300
Kaleh (1992) 305
Günther, Habermann (1994) 309
Frantzeskakis, Posonidis (2000) 316
An Initial Longitudinal Comparison 324
Multiple-Bit Differential Detection 326
Summary and Conclusions 344
Appendix: The Viterbi Algorithm 345

7 Detection in Frequency Selective Channels 1: Maximum Likelihood Detection 353
Problem Formulation 355
Maximum Likelihood Detection 356
The Viterbi Algorithm for Maximum Likelihood Sequence Detection 358
Summary and Conclusions 377

Interlude: Symbol-by-Symbol Detection Over ISI Channels 379

8 Detection in Frequency Selective Channels 2: Equalization 383
The Linear Equalizer 385
Problem Formulation 385
Equalizer Filter Coefficients: the MMSE Criterion . . 391
The Decision-Feedback Equalizer. 404
Problem Formulation 404
Equalizer Filter Coefficients: the MMSE Criterion . . 408
Summary and Conclusions 423

9 Detection in Frequency Selective Channels 3: Adaptive Equalization 425
The Adaptive Linear MMSE Equalizer 426
Variations on the LMS Algorithm 439
The Adaptive Decision-Feedback Equalizer 441

The Constant Modulus Algorithm: Blind Equalization . . 452
Summary and Conclusions 464

10 The Many Faces of Offset QPSK 467
A Variation on QPSK. 467
A Binary Modulation 471
A Version of CPM 472
OQPSK-Like CPM. 477
MSK 477
GMSK 484
SOQPSK-MIL 491
SOQPSK-TG 497
Cross-Correlated Trellis-Coded Quadrature Modulation (XTCQM) 502
Summary and Conclusions 514
Appendix: Continuous Phase Modulation 516
Signal Model 516
Detection 517
Laurent's Representation. 520

Bibliography 525

Index 561

Chapter 1

A Short History of Offset QPSK

Offset QPSK (OQPSK) has its beginnings at Bell Telephone Laboratories where the transmission of synchronous data streams on parallel channels was being investigated (Chang 1966; Saltzberg 1967; Chang et al. 1968). One way of producing parallel channels is to assign each channel to a different carrier frequency, usually with a fixed frequency spacing. The desire was to find as small a frequency spacing as possible. Of the many performance criteria investigated, one was cross talk between the parallel channels. It was thought that cross talk could be eliminated if the parallel channels were orthogonal. Investigations into orthogonality centered on the frequency spacing and the pulse shaping (Chang 1966). The modern reader instantly recognizes the ideas as a step in the development of orthogonal frequency division multiplexing (OFDM). It is tempting to read these articles in that way and overlook the techniques that came to be known as OQPSK. The first hint of OQPSK is buried in a footnote in (Chang 1966) where, given the channel spacings envisioned by Chang, the use of every other channel with non-aligned (delayed) symbol times makes it possible to achieve interchannel-interference-free transmission without the need for time-synchronous transmission across all the channels.

These ideas were developed further in (Saltzberg 1967). A block diagram of Saltzberg's system is illustrated in Figure 1.1. Each of the parallel channels has an inphase and quadrature component. Temporally synchronous data streams are presented to the system in parallel. Each of the parallel channels transmits two of the data streams, one on

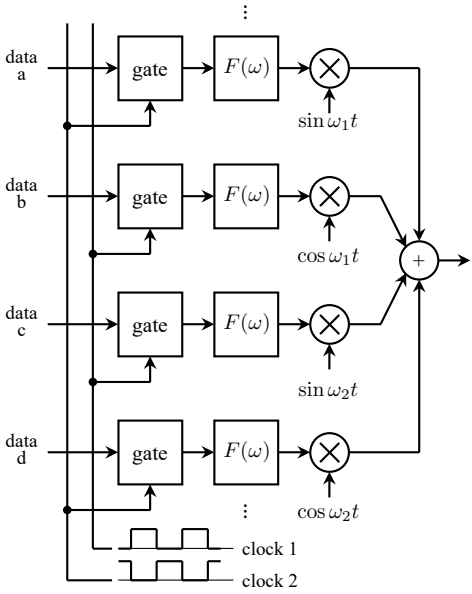

Figure 1.1: Saltzberg's system.

the inphase component and the other on the quadrature component. The signaling intervals on the inphase and quadrature components were offset by one half of a symbol time to improve bit error probability performance in dispersive channels. This is represented by the half-period offset in "clock 1" and "clock 2" in the figure.

A feature of Saltzberg's system that will play an important role below is the method used go generate the pulse trains. The data symbols are represented voltages at the left inputs to the "gate" blocks. The voltages are "gated" (a sample-and-hold operation) by a clock at the symbol frequency. The gating produces a pulse train with the non-return-to-zero (NRZ) pulse shape. To generate a more sophisticated pulse shape, the NRZ pulse train was applied to a continuous-time lowpass filter with frequency response $F(\omega)$. Given the technology of the day, this was the only practical option. The technology needed to apply digital signal processing to digital communications was more

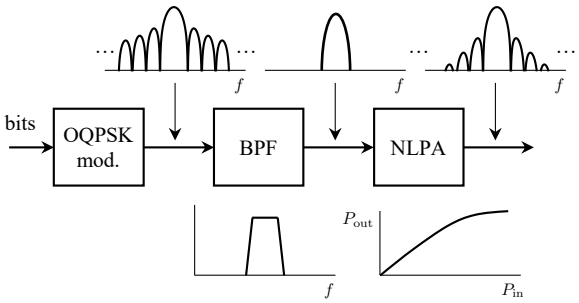

Figure 1.2: Kwan's system.

than two decades in the future.

The application that carried OQPSK to the present day was satellite communications. The first application of OQPSK in satellite communications was published in (Kwan 1969). Kwan's "double-binary PSK" is what is now called OQPSK. The main concern was the bit error probability degradation caused by hard limiting a filtered OQPSK signal. A block diagram of Kwan's system is shown in Figure 1.2. The system in the block diagram is typical of satellite transmitters at the time. As explained in the context of Saltzberg's system, it was relatively straightforward to generate OQPSK with NRZ pulse shape. Because the power spectral density of resulting waveform is a sinc-squared function, the resulting waveform had unacceptably poor spectral efficiency. To remedy this, a bandpass filter was applied. One way to interpret the operation is the removal of unwanted sidelobes by filtering. Another way to view the operation is that of changing the pulse shape to one that did not have undesired sidelobes. The bandpass filter in Figure 1.2 is equivalent to applying a pair of lowpass filters to the inphase and quadrature components of an NRZ OQPSK signal in Figure 1.1.

To close the satellite link the bandpass filter output had to amplified. The two properties of RF power amplifiers important to this telling of the history are the power efficiency and the input/output power characteristic. An RF power amplifier requires a power supply. The power supply, usually a DC voltage and corresponding DC current, must provide P_{DC} W to the RF power amplifier. The efficiency

is a measure of how well the RF power amplifier converts the DC power to RF power P_{RF}:

$$\text{efficiency} = \frac{P_{\mathrm{RF}}}{P_{\mathrm{DC}}}. \tag{1.1}$$

A closely related figure of merit is the power added efficiency

$$\text{power added efficiency} = \frac{P_{\mathrm{RF}} - P_{\mathrm{DC}}}{P_{\mathrm{DC}}}. \tag{1.2}$$

All satellites have severe size, weight, and power (SWAP) constraints. The SWAP constraints push the designer to apply an RF power amplifier in its most efficient mode.

The second property of interest is the input/output power characteristic. All RF power amplifiers exhibit a nonlinear input/output power characteristic. An example is shown in the figure below the block for the nonlinear power amplifier (NLPA). Chapter 2 presents two detailed examples.

Satellite systems were characterized by highly nonlinear RF power amplifiers (NLPAs). When a filtered signal is applied to an NLPA, the nonlinearities produced frequency content in the frequency bands occupied by the sinc-squared sidelobes. The reappearance of the unwanted sidelobes is called "spectral regrowth" (Rhodes 1972; Mathwich et al. 1974; Morais et al. 1980; Divsalar et al. 1982). Spectral regrowth does not occur with a linear power amplifier. At the time Kwan's paper was published, the only way to produce an RF power amplifier with a *linear* input/output power characteristic was to limit the instantaneous input power to a small values corresponding to the linear portion of the input/output power characteristic. This technique, called "backoff," reduced the transmit power which, in turn, reduced the carrier-to-noise ratio at the ground-based receiver.

The efficiency of the RF power amplifier is maximized when the RF output power is maximized. Increasing backoff reduces amplifier efficiency. This produced an efficiency/linearity tradeoff. For satellite systems, SWAP limitations motivate amplifier operation in a highly nonlinear mode. Bandwidth limitations motivate amplifier operation in a linear mode. Thus satellite systems presented the link designer with a tradeoff between bandwidth (via spectral regrowth) and carrier-to-noise ratio (via backoff).

Kwan examined this tradeoff for OQPSK. Curiously, Kwan does not state a motivation for OQPSK, nor does he compare the performance of OQPSK to non-offset QPSK. Kwan correctly attributed the bit error probability degradation to intersymbol interference (ISI) created by the nonlinear distortion of the NLPA.

The performance improvement realized by OQPSK relative to its non-offset counterpart was investigated in (Rhodes 1972). Rhodes' work showed that OQPSK experiences less spectral regrowth than QPSK. In a comparative study, (Taylor et al. 1976) showed that OQPSK significantly outperforms non-offset phase shift keying (PSK) over satellite channels using highly non-linear traveling wavetube amplifiers (TWTAs). Computer simulations were used to quantify the statistical properties of the amplitude fluctuations for OQPSK (and other modulations) caused by the BPF in (Greenstein and Fitzgerald 1979). OQPSK was shown to be less sensitive than QPSK to envelope fluctuations in (Moreno 1979). A new class of continuous-time bandpass filters was developed in (Bayless et al. 1979) and used to demonstrate that OQPSK and MSK (described below) have the lowest E_b/N_0 to achieve the bit error probability goal for nonlinearly amplified modulations in their comparison group. The design of the bandpass filter in Figure 1.2, constrained by an adjacent channel interference requirement, was examined in (Murakami et al. 1979). In satellite channels with cascaded nonlinear elements, (Fang 1981) showed that OQPSK and MSK (described below) outperform QPSK.

In the U.S., the transition from analog to digital technologies in the telephone system started on long-distance trunk links. As digital technology matured in the 1970s, the transition pace increased. Microwave line-of-site links were a key component in the long-distance network. Multipath fading is an important consideration in microwave line-of-site links. (Morais et al. 1979) showed that OQPSK is more sensitive than QPSK and 8PSK to amplitude distortion, but less sensitive to delay distortion. Because multipath fading introduces both amplitude and delay distortion, the winner was not clear. The analysis performed in (Greenstein and Prabhu 1979) concluded that the distortion produced by multipath fading degrades OQPSK more than QPSK. Later studies (Greenstein et al. 1982; Pahlavan 1985; Metzger et al. 1985) confirmed these conclusions. Despite this, (Morais et al. 1980) recommends OQPSK as the best choice for line-of-sight

microwave links given all the practical constraints. OQPSK appears to have been used on some microwave line-of-site links operated by AT&T (Giger et al. 1981).

The earliest work in synchronization was published in the 1970s. Rhodes investigated carrier phase synchronization derived from a noisy unmodulated residual carrier reference (Rhodes 1974). The results showed that OQPSK requires lower signal-to-noise ratio than QPSK. Simon derived and analyzed the decision-directed carrier phase PLL for OQPSK (Simon et al. 1974). Gitlin and Ho compared the impact of phase jitter on the bit error probability of QPSK and OQPSK and showed that OQPSK has superior phase jitter immunity and that the improvement is proportional to the waveform's excess bandwidth (Gitlin et al. 1975). Phase synchronization for duobinary encoded OQPSK was derived and analyzed in (Taylor and Cheung 1977). The first published examination of symbol timing synchronization for OQPSK was published (Lyon 1975). The impact of nonlinear power amplifiers on joint carrier phase and symbol timing synchronizers is described in (Palmer et al. 1980). A "demod-remod" tracking loop for carrier phase synchronization was described in (Weber et al. 1980a) and analyzed in (Weber et al. 1980b). (McBuffin et al. 1988) showed that OQPSK has the ability to correct inphase/quadrature reversals when impulsive noise injects a near 90° phase jump.

In joint decision-directed carrier phase and symbol timing phase lock loops, phase synchronization is achieved with a possibly non-zero static phase error. The static phase error is called a phase ambiguity. Carrier phase ambiguity resolution for OQPSK using correlators with unique words was first published in (Cacciamani et al. 1971). Differential encoding and decoding can also be used to solve the carrier phase ambiguity problem for OQPSK. The first published use of differential encoding in the OQPSK context is (Taylor and Cheung 1977). Taylor's differential encoder appears to be a special case of the duobinary encoder described in (Lender 1963). An alternative differential encoder and decoder was described in (Feher 1983). Feher's differential encoder appears to be a special case of Weber's general differential encoder (Weber 1978); the connection was made in (Rice 2007). The application of differential encoding to solve the phase ambiguity problem is described in Chapter 5.

By 1980, OQPSK was firmly established in satellite communica-

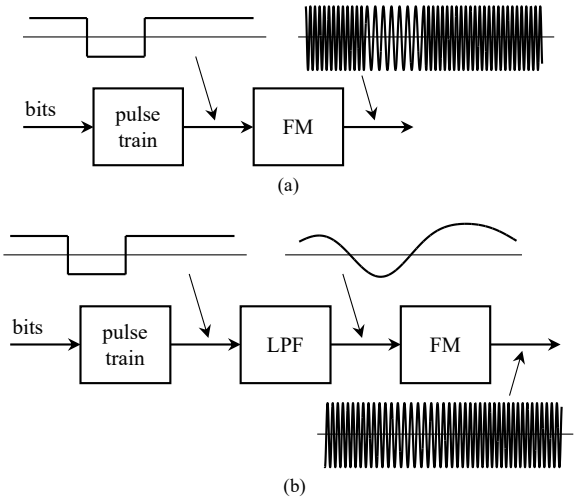

Figure 1.3: FM business (a) CPFSK; (b) with premod filter.

tions and was making its appearance in line-of-site microwave links. OQPSK's inclusion in the large surveys (Oetting 1979; Chakraborty et al. 1983) attests to this fact. OQPSK was selected as the modulation for the U.S. military telephone network AN/FRC-17x (Thomas et al. 1979) and used in the U.S. Army's tactical Radio Rely Set AN/GRC-144 (Bartow 1982) and in the U.S. defense satellite communications system (DSCS) (Gardner et al. 1986). The use of OQPSK in spread-spectrum multiple-access communications was described in (Garber et al. 1981; Elhakeen et al. 1982; Bartow 1982). In the context of secure military communications, (Reed et al. 1988) point out that a simple delay-and-multiply process can be used by an adversary to detect the symbol rate of (non-offset) QAM In contrast, the offset between the inphase and quadrature components of OQPSK make this process more difficult, thus producing a waveform that is less likely to be detected and identified by the adversary. Much later, a signal classifier based on the presence or absence of a timing offset between the inphase and quadrature components was published in (Liu et al. 2006).

Starting in the 1970's, spectrally efficient high data rate systems developed into a hot topic. A high data rate requires more transmit power whether the method for increasing the data rate is to reduce the symbol time for a low-order modulation or to adopt a high-order modulation. At the time, the high power amplifiers were still highly nonlinear and the spectral regrowth produced by the nonlinear characteristic presented a challenge to spectral efficiency.

It had been known for some time that frequency shift keying (FSK) does not experience spectral regrowth with nonlinear power amplifiers. This is because FSK has constant amplitude; a constant amplitude waveform is not distorted when passing through a nonlinear power amplifier. FSK may be produced by applying a properly scaled NRZ pulse train to an FM modulator. This is illustrated in Figure 1.3 (a). The technological limitations on pulse train generation described above apply here. The positive value on the pulse train produces a frequency shift of $+\Delta f$ Hz from the assigned carrier frequency; a negative value on the pulse train produces a frequency shift of $-\Delta f$ Hz. An example is shown in the figure. An FSK signal produced this way maintains a continuous phase during symbol transitions and was called continuous phase FSK (CPFSK). The bandwidth of the CPFSK signal is a nonlinear function of input pulse, Δf, and the input bit rate. The smallest value of Δf that renders orthogonal the two sinusoids at frequencies $f_c \pm \Delta f$ is $\Delta f = 1/4T_b$. CPFSK with the minimum orthogonal-preserving frequency shift is called minimum shift keying (MSK).

The earliest CPFSK systems used noncoherent detection, often in the form of a limiter-discriminator (an FM demodulator to the modern reader) followed by a timing synchronizer. The simplicity of nonlinear detection came at the cost of increased E_b/N_0 required to achieve the target bit error probability. Consequently, coherent detection was of interest. Because of the inherent memory in CPFSK, the maximum likelihood detector is a sequence detector, most often implemented as the Viterbi algorithm operating on a trellis. The complexity of the maximum likelihood sequence detector motivated the search for reduced complexity detection techniques with a small detection-efficiency penalty. The relatively good spectral efficiency of MSK made it the CPFSK of most interest.

Early on, it was recognized that there was a close connection be-

tween MSK and OQPSK with the half sine (HS) pulse shape. This was of great interest because of the promise that the maximum likelihood sequence detector could be replaced by a "linear detector" based on a much simpler OQPSK matched filter detector. The earliest published reference making the connection is (Sullivan 1972). A more thorough connection between the two was published in (Gronemeyer et al. 1976). The reduced complexity detector motivated by these connections was examined in (Amoroso et al. 1977). A nice summary of these results in presented in (Pasupathy 1979)

The impact on the power spectral density of MSK and OQPSK with the HS pulse shape in practical settings was published in (Mathwich et al. 1974). The comparative studies reported in (Taylor et al. 1976; Taylor, Ogletree, et al. 1977) showed that a closely related modulation known as fast frequency shift keying (FFSK) experiences slightly less bit error probability degradation than OQPSK with the HS pulse shape in a satellite channel using a highly non-linear TWTA. The FFSK advantage was slight and was only observed at small values of the bandwidth symbol time product BT. As BT increased, OQPSK had the slight advantage. The analysis presented in (Matyas 1978) showed that FFSK performs better than OQPSK in the presence of a noisy phase reference. In all investigations of digital modulation over nonlinear channels, the performance of OQPSK is equivalent to that of MSK, and both OQPSK and MSK exhibit better performance than (non-offset) QPSK (Bayless et al. 1979; Fang 1981; Austin et al. 1983).

A closely-related effort sought to maximize the number of asynchronous digitally modulated signals frequency multiplexed into a given bandwidth. One of the performance measures was time-domain "cross talk" between adjacent channels. OQPSK was compared to (non-offset) PSK and MSK in (White 1977; Kalet 1977; Reiffen et al. 1978). The published results were consistent: MSK outperformed the others.

Motivated in part by the success of the connection between HS OQPSK and MSK, generalizations were explored. A first attempt was to consider band limiting MSK, using a post-modulator band pass filter, to improve spectral efficiency. Bandlimiting a constant envelope signal produces amplitude variations—it is the amplitude variations that produce spectral regrowth at the output of a nonlin-

ear amplifier. This approach was examined in (Mathwich et al. 1974) for the case where a highly nonlinear power amplifier was applied to the filtered MSK signal. The results showed that if the band limiting was not too aggressive, the detection efficiency loss was 1 dB or less. The next step was generalize the pulse shape: replace the HS pulse shape with a more bandwidth efficient pulse shape subject to the constant envelop constraint (Simon 1976). Simon derived a set of conditions the pulse shapes (or "modulating pulses" as he called them) must meet. A more general class of pulse shapes achieving these goals were developed in (Rabzel et al. 1978). The conclusion in (Cruz et al. 1980) is that improvements beyond those in (Amoroso 1976; Simon 1976; Rabzel et al. 1978) require investigation of other modulation techniques. The temporal raised-cosine shape was incorporated into OQPSK in (Austin et al. 1981) to produce what was called "quadrature overlapped raised-cosine (QORC) modulation." Austin and Chang showed the QORC possesses the benefits of both OQPSK and MSK. Other approaches to producing time-limited pulses for OQPSK were published in (Beaulieu et al. 1992; Vigil et al. 1995).

The question for constant envelope signals with improved spectral efficiency followed two parallel paths. Along one path the pulse shaping used for OQPSK was generalized. Instead of using one pulse to create the pulse train, a *set* of pulses was envisioned. Pulse pairings in the inphase and quadrature components were constrained to create waveform segments with a constant envelope. Most of this work was performed in the 1980s. Noteworthy contributions on this path include (Le-Ngoc et al. 1982; Kato et al. 1983; Sasase et al. 1984; Sasase, Nagayama, et al. 1985; Sasase, Feher, et al. 1985; A. Gusmão et al. 1988, 1990; Rasmussen et al. 1993; F. Lin et al. 1993; Wyskiel et al. 1992; Gusmão et al. 2008). Some representative examples are explored in Chapter 10.

The other path involved generalizations to MSK. The approach is illustrated in Figure 1.3 (b). A lowpass filter—called a premodulation filter in this context—was applied to the NRZ pulse train. This is the same approach used in Saltzberg's system in Figure 1.1 to generate a pulse train with a more sophisticated pulse shape. Because signal is a form of FSK, it has constant envelope. In the resulting real-valued bandpass waveform shown in the figure, the transition from thef high frequency to the low frequency is barely perceptible. This is in con-

trast to the abrupt, but phase-continuous, transition in the waveform shown in Figure 1.3 (a) for the same value of Δf. The smoother frequency shift is a result of the smoothing applied to the pulse train by the premodulation filter. Smoother frequency shifts reduce the bandwidth of the frequency modulated signal. The bandwidth reduction was achieved at the cost of detector complexity: the lowpass filter introduces ISI in the pulse train. The ISI increases the memory order of the modulated carrier. The increased memory order increases the size of the trellis used by the sequence detector. The premodulation filter that gained the most traction was the lowpass filter with a Gaussian impulse response first published in (Murota et al. 1981) and called Gaussian minimum shift keying. The "minimum shift keying" part of the name follows from the use of the same frequency shift used for MSK and the "Gaussian" part of the name describes the impulse response of the premodulation filter.

In the 1980s work began on a pan-European digital cellular standard. The *Groupe Spécial Mobile* (GSM) committee developed the technical standard that later bore its name. A slightly modified version of the GSM standard was used for the personal communications service (PCS) in the U.S. GSM adopted GMSK as the modulation (Mouly et al. 1992). The reasons for the adoption are those discussed above: constant envelope for use with a nonlinear RF power amplifier and good spectral efficiency.

The GMSK detector has many features on common with an O-QPSK detector. The real and imaginary parts of the complex-valued lowpass equivalent signal are sampled at symbol-spaced intervals offset by one-half symbol time. For an OQPSK signal using an ISI-free pulse shape, decisions are made from the samples on a symbol-by-symbol basis. The same symbol-by-symbol detector (with provisions for 90-degree rotations each bit time) was described in the original GMSK article (Murota et al. 1981). However the bit error probability performance can be limited by the ISI introduced by the premodulation filter. indexContinuous phase modulation (CPM)!premodulation filter To address the performance limitation, the OQPSK symbol-by-symbol detector is replaced by a sequence detector. A rudimentary sequence detector was described in (Ishizuka et al. 1984).

At the same time, a common mathematical framework for CPFSK, MSK, and GMSK and other variations of "digital FM" was developed

in (Aulin and Sundberg 1981; Aulin, Rydbeck, et al. 1981). The articles showed that CPFSK, MSK, and GMSK, are special cases of what the authors coined continuous phase modulation (CPM). Frequency pulses are normalized to area 1/2. Frequency pulses with duration one symbol symbol time produce full response CPM; frequency pulses with duration multiple symbol times produce partial response CPM. The digital modulation index was defined as $h = 2\Delta f T_s$. Thus MSK a full response CPM with $h = 1/2$; GMSK is a partial response CPM with $h = 1/2$.

The connection between CPM with $h = 1/2$ and OQPSK was explained above. The mathematical underpinnings of this connection were formalized in (Laurent 1986). In Laurent's representation, CPM is written as a sum of parallel pulse trains. Each of the pulse trains use a different pulse. The weights applied to the pulses are pseudo-symbols. The special case of MSK produces one pulse train with HS pulse shape and pseudo-symbols that are related to the binary symbol values by 90-degree rotations. The result is OQPSK with the HS pulse shape with a form of differential encoding. For GMSK, using only one of the parallel pulse trains in the detector gives rise to an OQPSK-like symbol-by-symbol detector. Basing a detector on a subset of the pulse trains (usually the strongest) in Laurent's decomposition was first published and analyzed by (Kaleh 1989a), The application of Kaleh's approach to GMSK was described and analyzed in (Kaleh 1989a; Al-Dhahir et al. 1998).

An extensive comparison involving M-ary PSK, OQPSK, and CPM was carried out in (Rapp 1990) for radio links characterized by nonlinear power amplifiers and adjacent channel interference (ACI). Rapp's conclusions followed two fronts: (1) The nonlinear power amplifier caused no degradation for CPM, only modest degradation for OQPSK, and "tolerable" degradations for MPSK as long as the nonlinear power amplifier point was correctly chosen; and (2) CPM and OQPSK degraded more quickly than MPSK as ACI increased. Because computational complexity of the MPSK detector is much less than that of the CPM detector, Rapp conjectured that linearized nonlinear power amplifiers (usually accomplished via predistortion) with coded MPSK was the path forward. In a comparison of modulations for millimeter wave frequencies, OQPSK was the recommended choice (Gulloch et al. 1993).

First generation cellular telephony in the US used analog FM for the uplink and downlink. The goal of second generation cellular telephony in the US was to improve spectral efficiency. This was accomplished by adopting a digital modulation. Deliberations on the modulation focused on the need for good performance through nonlinear power amplifiers and the ability to use differential detection in propagation environments with rapidly fluctuating phase offsets. OQPSK was the obvious choice, but the absence of a differential detection algorithm with good performance for OQPSK motivated the adoption of a compromise modulation called $\pi/4$-QPSK and its differentially-encoded version $\pi/4$-DQPSK (Günther et al. 1994; Hischke et al. 1997; Hischke et al. 1998b). $\pi/4$-QPSK is described in Chapter 2 (see pp. 33 ff) and can be conceptualized as the superposition of two QPSK constellations, one shifted by $\pi/4$ radians relative to the other. The transmitted symbols alternate between the two constellations. Because of the $\pi/4$ phase shift between the two constellations and the alternation between them, the phase trajectory of $\pi/4$-QPSK does not pass through the origin thus reducing the envelope fluctuations in a manner similar to, but not as good as, OQPSK. $\pi/4$-DQPSK was adopted in the US digital cellular standard (Chennakeshu et al. 1993), the Japanese digital cellular system (Günther et al. 1994; Hischke et al. 1997), and the Trans European Trunked Radio (TETRA) system (Günther et al. 1994; Hischke et al. 1997).

The absence of a differential detector with good performance of OQPSK motivated the search for one. At the time $\pi/4$-QPSK was adopted in the systems described in the previous paragraph, the only differential detection algorithms for OQPSK were due to (Defly et al. 1989) and (Kaleh 1989a). Kaleh's system was based on an equalizer to address the ISI caused by the time delay between inphase and quadrature components of OQPSK. This equalizer worked well for MSK (= OQPSK with the HS pulse shape) but failed with the NRZ and filtered NRZ pulse shapes. Motivated by this shortcoming, Kaleh developed a differential detector based on a sequence detector to address the ISI in (Kaleh 1992). The trellis used in Kaleh's system was based on the differential encoding that characterizes the relationship between MSK and OQPSK. A differential detector based on the more conventional differential encoding was developed in (Günther et al. 1994; Hischke et al. 1997). The differential detector used a se-

quence detector operating on a 16-state trellis. A different approach was adopted in (Frantzeskakis et al. 1999; Frantzeskakis et al. 2000); samples of the instantaneous phase difference were used to develop a sequence detector operating on an 8-state trellis. Günther's differential detector and Frantzeskakis' differential detectors were the best performing differential detectors, but the bit error probability performance of both was about 2 dB inferior to that of fully coherent detection of differentially-encoded BPSK (see Figure 6.20 in Chapter 6). To close the gap, multiple-bit differential detectors were explored by (Simon 2003; Phoel 2004; Schober et al. 2005). Schober's system was able to close the performance gap was the block length increased. The technical details of these differential detectors are summarized in Chapter 6.

The nature of then future wireless networks generated interest in burst-mode communication techniques starting in the 1990's. The initial work focused on burst-mode communications for satellite systems (Seki et al. 1992; Kobayashi et al. 1992; Jiang et al. 1999) and later for terrestrial mobile radio networks (Hischke et al. 1998a; Morawski et al. 1999; D'Amico et al. 1999). Burst mode communications are usually coupled with time-division multiple access (TDMA) wherein multiple users are assigned to the same frequency, but communicate in different time slots. The primary technical interests in burst-mode applications are burst detection and synchronization. For both, rapid acquisition is paramount.

One effort to increase the spectral efficiency of OQPSK was to apply the temporal offset to M-ary QAM for $M > 4$. This was called offset QAM or (OQAM). The idea was explored for digital broadcast television in (Ohnishi et al. 1989), personal communications systems (Chuang 1989; Malkamäki 1992), and satellite communications (Kobayashi et al. 1992). An mathematical analysis of the probability of bit error performance of OQAM was carried out in (Oshita et al. 1989). Frequency-domain equalization techniques for OQAM were developed and analyzed in (Luzio et al. 2010a, 2011).

Two comparative studies were devoted exclusively to land mobile satellite channels (Lodge et al. 1987; Belce 2003). Of the modulations considered by Lodge, OQPSK with differential detection was the best solution. In Belce's study, QPSK, OQPSK, and MPSK with coherent detection were compared with $\pi/4$-QPSK with non-coherent

detection. The bit error probability degradation of $\pi/4$-QPSK in the presence of fading and Doppler shifts was less than that of the others, but due to noncoherent detection, the nonfaded performance of $\pi/4$-QPSK was not as good. The author of this book conjectures that had Belce applied differential detection to OQPSK, the conclusions would have been different.

With the interest in OQPSK for mobile wireless networks, detection in multipath propagation environments became an intense area of investigation. Maximum likelihood sequence detection of OQPSK in ISI channels is developed in Chapter 7. Filter-based equalization techniques were developed in (Bello et al. 1984; Gudmundson 1988; Tu 1993; Craig 1993; Wales 1994; López-Valcarce 2002; Gerstacker et al. 2003; Raphaeli 2010). Filter-based equalizers are examined in Chapter 8 (fixed equalizers) and Chapter 9 for adaptive equalizers. Frequency-domain equalization of OQPSK has been investigated by Rui Dinis and his team in (Montezuma et al. 2009; Luzio et al. 2009; Dinis et al. 2010; Luzio et al. 2010b, 2010a, 2011; Luzio, Dinis, Montezuma, et al. 2012; Luzio, Dinis, and Montezuma 2012, 2013, 2014).

Accompanying the development of equalization techniques for multipath channels, synchronization techniques for multipath fading channels were also published. Timing synchronization for frequency nonselective fading channels was investigated in (Bucket et al. 1994a), The impact of non-ideal interpolation on carrier phase synchronization over frequency non-selective fading channels was studied in (Bucket et al. 1994b). Sequences to enable mobile channel estimation for use with OQPSK were published in (Popović 1995). A method for blind carrier phase synchronization in time-selective fading channels for OQPSK was described in (Ghogho et al. 1999).

"Digital Modems"—modulators and demodulators using discrete-time signal processing—that supported OQPSK began to appear in the 1990s. The programmable digital modem for satellite systems was described in (Poklemba 1992). The effect of non-ideal interpolation (in the timing synchronizer) on carrier phase synchronization in digital models was investigated in (Bucket et al. 1994b).

In the 1990s advancement in satellite technologies included OQPSK. Digital video transmission via satellite was examined in (Kubota et al. 1989; Kubota et al. 1992; Kato et al. 1992), NASA's experimental Advanced Communications Technology Satellite (ACTS) supported

OQPSK (Bergamo et al. 1995; Acosta et al. 1999). A comparative study of the performance of a detect/remodulate satellite payload (Majeed et al. 1997) concluded OQPSK was best suited to the application. An OQPSK satellite modem using the then latest technology was described in (Zhao et al. 2004). For space communications, NASA's Spacecraft Transponding Modem supported OQPSK (Berner et al. 2000).

A renewed effort to both understand and *exploit* the nonlinear transmission medium where OQPSK shines was also undertaken. Notable modeling techniques motivated by OQPSK include (Metzger et al. 1996) who showed that reducing adjacent channel interference in OQPSK is accomplished at the expense of increased ISI; and practical models in (Struble et al. 1997; A. Gusmão et al. 1997). This line of inquiry culminated in (Montezuma et al. 2010b, 2010a) who showed that coded OQPSK followed by a nonlinearity can be modeled as a serially-concatenated coding scheme. Properly designed codes can improve performance.

Direct sequence (DS) spread spectrum began seeping into the public domain in the late 1980s after years of obscurity in classified military projects. Direct sequence spread spectrum is the underlying technology for direct sequence code division multiple access (DS-CDMA) wherein users share the same spectrum at the same time, but are assigned different spreading codes. It did not take long for CDMA and OQPSK to be paired: the advantages of OQOSK with DS-CDMA for tactical radios was published in (Rasmussen et al. 1992). The advantages identified by Rasmussen are those described above: the reduction of spectral regrowth for nonlinearly amplified RF signals. Rasmussen described a slight modification to OQPSK to permit serial demodulation.

A DS-CDMA standard for second generation cellular telephony in the US was published in 1995 by the Telecommunications Industry Association as Interim Standard 95 (IS-95). Direct sequence spread spectrum was a competing option for second generation cellular telephone system in the US. The appeal was the good performance of spread spectrum over frequency selective propagation channels and the ability to apply multiuser detection techniques. The application of OQPSK to the IS-95 system appeared in (Sugiyama et al. 1994; Sugiyama et al. 1995).

The techniques published in the 1990s relied heavily on discrete-time signal processing (often called "digital" signal processing—DSP). They were part of a larger trend in wireless communications enabled by improvements in DSP technology that prompted the development of more sophisticated sampled-data solutions for wireless communications.

In the 2000's, many of the trends started in the 1990s continued. More theoretical analyses of synchronization methods for OQPSK appeared in (Riba et al. 1998; Hong et al. 2000; Gifford et al. 2000; López-Valcarce 2002; López-Salcedo et al. 2004; López et al. 2006; Simon 2006; Rice et al. 2009; D'Amico 2015), OQPSK was incorporated into modems for deep space communications (Kinman et al. 2002), OQPSK was considered for use in the 60 GHz band in (Nsenga et al. 2007), and continued advances in DS CDMA were published in (Landolsi et al. 2002b, 2002a; Song et al. 2003; Mirbagheri et al. 2004, 2006; Sood et al. 2008).

OQPSK was also applied in new ways. OQPSK was adopted in the 2006 revision of the IEEE 802.15.4 standard for low-rate wireless personal area networks in the 868.0–868.6 MHz band (Europe) and 902-928 MHz band (US). The use of OQPSK in multiple-input multiple output (MIMO) systems using space-time coding was described in (Nelson et al. 2004; Jensen et al. 2005; Anderson et al. 2005; Nelson et al. 2006, 2007; Dang et al. 2008; Rice et al. 2010). The interesting feature is detection with space-time block coding. For non-offset modulations using a space-time block code, the optimum detection is performed on a block-by-block basis. In contrast, optimum detection of OQPSK with a space-time block code is a sequence detector. The reason for this is the temporal offset between the inphase and quadrature components (Rice et al. 2010).

In a departure from RF communications, the application of O-QPSK in optical communications was described in (Shao, Chi, Li, Zhou, et al. 2009; Shao, Chi, Li, Hou, et al. 2009; Cai 2009; Detwiler et al. 2010) and for printed wiring board channels in (Yeo et al. 2007; Yeo et al. 2008). Yeo's work focused on high-bandwidth, low-cost transceivers for applications such as backplane connections. In these applications, low cost requires nonlinear amplifiers. Because OQPSK produces less spectral regrowth, the bandlimiting nature of the channel introduces less distortion than baseband PAM systems using the

NRZ pulse shape. The "carrier frequency" in Yeo's system is set of one-half the symbol rate. OQOSK for underwater communications is explored in (Waldhorst et al. 2001).

Of all the new applications, the most interest has been the use of OQPSK with multicarrier systems such as orthogonal frequency division multiplexing (OFDM) and filterbank multicarrier (FBMC) modulation: (Chen et al. 1997; Nedić 2000; Bölcskei et al. 2001; Bellanger et al. 2002; Ciblat et al. 2004; Mongol et al. 2005; Azarnasab et al. 2007; Fusco et al. 2007; Javaudin et al. 2007; Zhang et al. 2008; J. Lin et al. 2009; Bellanger 2008b, 2008a; Fusco, Izzo, et al. 2008; Fusco, Petrella, et al. 2008; Garbo et al. 2008b, 2008a, 2008c; Goljahani et al. 2008; Kunishima et al. 2008b, 2008a; Fusco, Petrella, et al. 2009a, 2009b, 2009c; Fusco, Izzo, et al. 2009; Ikhlef et al. 2009; J. Lin et al. 2009; Zhang et al. 2009; Bellanger et al. 2010; Caus and Pérez-Neira 2010; Caus and P/'erez-Neira 2010; Dandach et al. 2010c, 2010a, 2010b; Dhuness et al. 2010; Zakaria et al. 2010; Caus et al. 2011b, 2011a, 2011c; Dandach et al. 2011; Rocha et al. 2011; Ihalainen et al. 2011; Caus, Pérez-Neira, and García-Armada 2012; Caus and Pérez-Neira 2012a, 2012b, 2012c; Mattera et al. 2012, 2013; Caus and Pérez-Neira 2013b; Caus, Pérez-Neira, and Moretti 2013; Caus and Pérez-Neira 2013a, 2014; Caus, Pérez-Neira, Moretti, and Kliks 2014; Pérez-Neira et al. 2015; Caus et al. 2015; Savaux et al. 2016; Caus et al. 2016; Nissel and Rupp 2016c, 2016a; Nissel, Caban, et al. 2016; Nissel and Rupp 2016b; Pérez-Neira et al. 2016; Nagy et al. 2017; Nissel, Zöchmann, et al. 2017b, 2017a; Nissel and Rupp 2017; Nissel, Blumenstein, et al. 2017; Nissel, Rupp, and Marsalek 2017; Nissel, Schwarz, et al. 2017; Sakai et al. 2017; He et al. 2018; Nissel et al. 2018; Nisssel et al. 2018; Singh et al. 2018, 2019; Kataksham et al. 2023)

OFDM was adopted as the modulation for digital audio broadcasting (DAB) in 1997, digital terrestrial television broadcasting (DVB) in 1997, asymmetric digital subscriber lines (ADSL) in 1998, and for 802.11 "Wi-Fi" in 1999. For mobile wireless applications, the propagation channel may be modeled as a linear time-varying system. In such cases, OFDM experiences both temporal and frequency dispersion. This dispersion erodes the orthogonality of the time-frequency basis functions which, in turn, reduces the probability of bit error performance. Pulse shaping can help "localize" the time-frequency basis

functions, but the localization is often achieved at the expense of spectral efficiency. Motivated by the work of Chang and Saltzberg that opened this Chapter, Bölcskei showed that delaying the quadrature component of the OFDM symbol by one-half symbol time relative to the inphase component reduces the impact on spectral efficiency by the pulse shaping (Bölcskei et al. 2001).

Cellular telephony's Long Term Evolution (LTE) was adopted as the migration path from second and third generation systems to fourth generation systems. LTE was first proposed in the late 1990s and was adopted as a cellular telephony standard in late 2008. LTE uses OFDM as the RF modulation and is therefore incompatible with the RF modulations used in second and third generation systems.

Offset QAM is particularly attractive for FBMC modulation. In OFDM, QAM symbols modulate each subcarrier using the inverse fast Fourier transform (IFFT) algorithm. The IFFT preserves orthogonality between the subcarriers, but produces a wave form with relatively high out-of-band emissions, high peak-to-average power ratio, and requires a cyclic prefix to enable frequency domain equalization. For channels with large delay spreads, the inclusion of the cyclic prefix reduces spectral efficiency. FBMC modulates each carrier using an FIR filter. The subcarrier filters are usually arranged in a filterbank to reduce implementation complexity. The filterbank improves spectral efficiency over OFDM by reducing out of band emissions and eliminating the need for the cyclic prefix. These benefits are achieved at the cost of increased complexity and the loss of subcarrier orthogonality: the subcarriers interfere with each other in both time and frequency. The orthogonality issue is addressed by delaying the quadrature component of the subcarrier by one-half symbol time relative to the inphase component. With a properly designed subcarrier filter, the matched filter output exhibits no interference in the inphase component of its output: all the interference is concentrated in the quadrature component.

The rationale for combining offset modulation with FBMC brings the history back to its starting point. Interference suppression on parallel channels (in this case the inphase and quadrature channels) is reduced by staggaring the transition times on the two channels. Along the way, it was realized that the temporal offset between the inphase and quadrature components reduced envelope fluctuations.

Reduced envelope fluctuations reduce spectral regrowth at the output of a nonlinear power amplifier. Because satellite transponders used highly nonlinear power amplifiers, OQPSK quickly found a home in satellite communication systems. Along with the benefits, the timing offset also made some things more challenging, such as channel estimation, differential detection, and equalization.

The history of OQPSK offers a glimpse into the broader history of digital communications. The detection and synchronization techniques evolved from the limitations of continuous-time circuits to advanced techniques in DSP. The evolution of analog-to-digital converters, increasing clock rates of programmable processors, and the shrinking size of VLSI all contributed to the trend. OQOSK is not the answer to every need in digital communications. But, in the applications where it shines, it is hard to beat.

Chapter 2

Description and Properties

Preliminaries

Offset QPSK (OQPSK) is almost exclusively used as a real-valued bandpass signals. For this reason, the relationship between a real-valued bandpass signal $s_{\mathrm{BP}}(t)$ and its corresponding complex-valued lowpass equivalent $s(t)$ are of interest.

A bandpass signal $s_{\mathrm{BP}}(t)$ is a signal whose Fourier transform $S_{\mathrm{BP}}(f)$ is positioned about a frequency $f_0 \gg 0$. The bandpass signal $s_{\mathrm{BP}}(t)$ is real-valued if its Fourier transform is symmetric: $S_{\mathrm{BP}}(f) = S_{\mathrm{BP}}(-f)$. Consequently, the Fourier transform of a real-valued bandpass signal must have a mirror image at $-f_0$. An example is shown in Figure 2.1 (a). The figure shows f_0 in center of $S^+_{\mathrm{BP}}(f)$, but this does not have to be the case.

The Complex-Valued Lowpass Equivalent Signal in Terms of the Real-Valued Bandpass Signal: The expression for $S(f)$, the complex-valued lowpass equivalent of $S_{\mathrm{BP}}(f)$, starts with the analytic or pre-envelope signal $S^+_{\mathrm{BP}}(f)$. The analytic signal is the positive frequency component of the bandpass signal:

$$S^+_{\mathrm{BP}}(f) = S_{\mathrm{BP}}(f)u(f) \tag{2.1}$$

where $u(\cdot)$ is the unit step function. $S(f)$ is two times the frequency translated analytic signal

$$S(f) = 2S^+_{\mathrm{BP}}(f + f_0) = 2S_{\mathrm{BP}}(f + f_0)u(f + f_0). \tag{2.2}$$

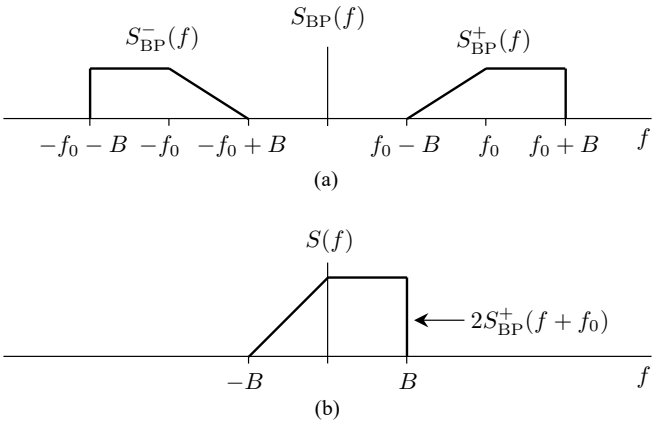

Figure 2.1: Frequency-domain representations: (a) a real-valued bandpass signal; (b) the corresponding complex-valued lowpass equivalent signal.

An example of $S(f)$ is shown in Figure 2.1 (b). The Fourier transform shown in the figure is positioned about $f = 0$. Thus $s(t)$, the inverse Fourier transform of $S(f)$, is a lowpass signal. If $S_{\mathrm{BP}}(f)$ is symmetric about f_0, then $S(f)$ is symmetric about $f = 0$ and the corresponding time-domain signal $s(t)$ is real valued. Otherwise, $s(t)$ is complex valued. This is the case shown in the figure.

In the time domain, the analytic signal is

$$s^+_{\mathrm{BP}}(t) = \frac{1}{2}s_{\mathrm{BP}}(t) + j\frac{1}{2}\hat{s}_{\mathrm{BP}}(t) \tag{2.3}$$

where $\hat{s}_{\mathrm{BP}}(t)$ is the Hilbert transform of $s_{\mathrm{BP}}(t)$:

$$\hat{s}_{\mathrm{BP}}(t) = s_{\mathrm{BP}}(t) \star \frac{1}{\pi t}. \tag{2.4}$$

Applying the frequency translation property of the Fourier transform to (2.2) gives the time-domain representation

$$s(t) = 2s^+_{\mathrm{BP}}(t)e^{-j2\pi f_0 t} = \left[s_{\mathrm{BP}}(t) + j\hat{s}_{\mathrm{BP}}(t)\right] e^{-j2\pi f_0 t}. \tag{2.5}$$